BIOCHEMISTRY
including biophysical chemistry & molecular biology

Article

pubs.acs.org/biochemistry

Whole Cell Nuclear Magnetic Resonance Characterization of Two Photochemically Active States of the Photosynthetic Reaction Center in Heliobacteria

Smitha Surendran Thamarath,[†] A. Alia,[†] Eugenio Daviso,[†,§] Deni Mance,[†] John H. Golbeck,*[,‡] and Jörg Matysik*[,†]

[†]Leiden Institute of Chemistry, Leiden University, Einsteinweg 55, 2300 RA Leiden, The Netherlands

[‡]Department of Biochemistry and Molecular Biology and Department of Chemistry, Pennsylvania State University, 328 South Frear Laboratory, University Park, Pennsylvania 16802, United States

Supporting Information

ABSTRACT: Applying photo-CIDNP (photochemically induced dynamic nuclear polarization) MAS (magic-angle spinning) nuclear magnetic resonance to whole cells of *Heliobacillus (Hb.) mobilis*, we demonstrate that heliobacterial reaction centers are operational in two different states as indicated by the occurrence of a light-induced spin-correlated radical pair. A culture maintained anaerobically is called "Braunstoff" (German for "brown substance"). After exposure to oxygen, Braunstoff is converted to "Grünstoff" ("green substance") as indicated by a color change due to the conversion of BChl *g* to Chl a_F. It is shown that electron transfer occurs symmetrically via both branches of cofactors in both forms. The donor and acceptor cofactors remain identical and unchanged upon conversion, while the intermediate accessory cofactors are transformed from BChl *g* to Chl a_F. The donor triplet state in Braunstoff is localized on the special pair donor and lives for 100 μs, demonstrating the absence of nearby carotenoids. In Grünstoff, the donor triplet becomes mobile and appears to be formed on an accessory cofactor.

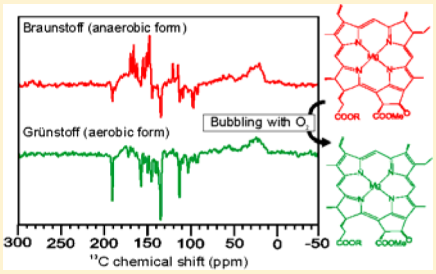

Heliobacillus (Hb.) mobilis is a strictly anaerobic, nitrogen-fixing photosynthetic organism found in abundance in rice paddy fields.[1−3] The photosynthetic machinery of *Hb. mobilis* contains antenna pigments and most of the reaction center (RC) cofactors bound to a single polypeptide dimer in the cytoplasmic membrane. *Hb. mobilis* has a type I RC as defined by the presence of iron−sulfur cluster F_X as a bound electron acceptor.[4] Because it is a homodimer and has a simple polypeptide composition, the heliobacterial RC has been proposed to be the evolutionary ancestor of photosystem I (PS I).[5,6] The more complex heterodimeric PS I may thus have evolved by a simple gene duplication event.[7] Unlike other photosynthetic bacteria, *Hb. mobilis* contains few complex structures such as intercytoplasmic membranes and has no chlorosomes.[1,8] Because of its simple polypeptide composition, the heliobacterial RC is an ideal model for understanding structure−function relationships within homodimeric RCs.[3] Thus far, however, there is no structural information available for any homodimeric type I RC.

The absorption spectrum of anaerobic *Hb. mobilis* cells is shown in Figure 1 (red spectrum). The color appears brownish green and is therefore called "Braunstoff". A unique pigment, bacteriochlorophyll *g* [BChl *g* (see Figure 2A)], has been identified in these bacteria.[9] BChl *g* acts as antenna pigment, and two 13^2 epimers (BChl *g*′) act as the primary electron donor special pair ($P798^+$).[10] The primary electron acceptor is 8^1-hydroxychlorophyll *a* [8^1-OH Chl a_F (Figure 2B)]. The

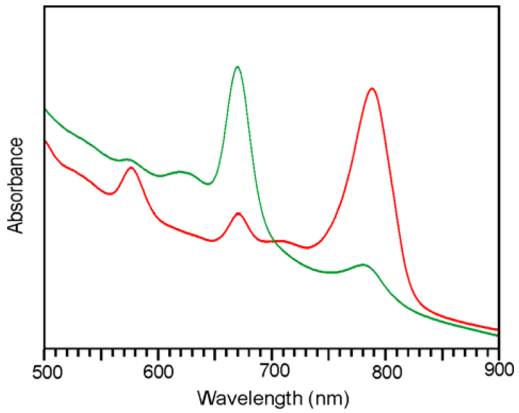

Figure 1. Absorption spectra of heliobacterial cells in the anaerobic (Braunstoff, red) and aerobic (Grünstoff, green) states. The absorbance is presented in arbitrary units.

intense absorbance peaks at 570 and 798 nm correspond to BChl *g*. The less intense peak at 670 nm corresponds to 8^1-OH Chl a_F.[11] Both isolated RCs and membranes have been studied by FT-IR,[12] EPR techniques,[13] and photo-CIDNP MAS NMR.[14] A peculiarity of BChl *g* is the photoconversion at

Received: April 12, 2012
Revised: June 28, 2012
Published: July 2, 2012

   dx.doi.org/10.1021/bi300468y | *Biochemistry* 2012, 51, 5763−5773

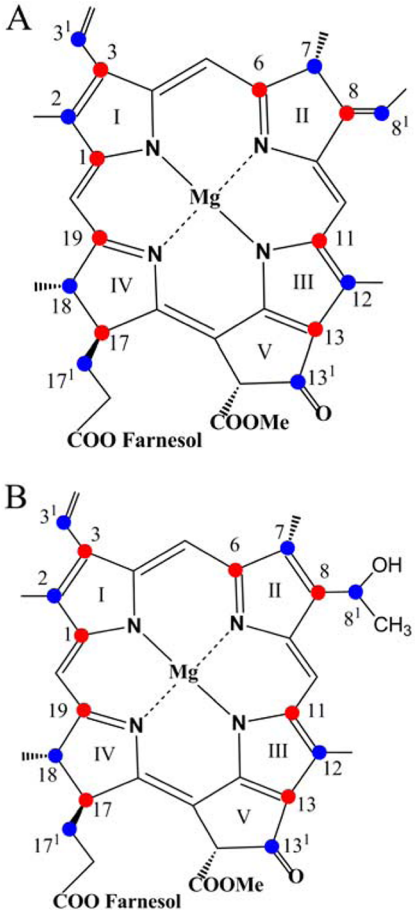

Figure 2. BChl *g* (A) and 8^1-OH BChl *a* (B) with label patterns obtained by feeding 4-Ala (red) and 3-Ala (blue).

pyrrole ring II when BChl *g* exposed to oxygen in the presence of light. The change in color from brownish green to emerald green is observed during this process and leads to a product called Grünstoff. The pigment becomes spectroscopically equivalent to Chl *a*, which is present in cyanobacteria and green plants. The absorption spectrum of *Hb. mobilis* after this process is shown at Figure 1 (green spectrum). The magnitudes of all absorbance peaks of the BChl *g* pigment decrease. The small remaining peak at 798 nm indicates that the conversion is not quantitative. The peak at 670 nm, indicating Chl a_F, becomes more intense. There is not much information available about Grünstoff other than its absorption spectrum. Here, both Braunstoff and Grünstoff are studied by ^{13}C and ^{15}N photo-CIDNP MAS NMR directly at the cellular level. We demonstrate that in heliobacterial RCs under aerobic conditions, radical pairs are also formed in Grünstoff by light-induced electron transfer.

The solid-state photo-CIDNP effect, discovered in 1994 by Zysmilich and McDermott,[15] has been observed in all natural RCs studied, and it has been assumed that the effect is an intrinsic property of light-induced electron transfer in photosynthesis.[16] In this effect, the non-Boltzmann nuclear spin polarization is detected as a strongly enhanced ^{13}C or ^{15}N MAS NMR signal.[17] The non-Boltzmann spin distribution is achieved by the transfer of the electron spin polarization from the primary radical pair to the nuclear spins by hyperfine interaction.[18] Such transfer at the high magnetic fields as applied in an NMR experiment is explained by one or more of three parallel mechanisms that occur in the solid state under conditions of continuous illumination:[19−21] three-spin mixing (TSM),[22] differential decay (DD),[23] and differential relaxation (DR).[24]

These mechanisms are well understood in photo-CIDNP MAS NMR studies of the quinone-removed RCs of *Rhodobacter sphaeroides* and in theoretical simulations based on these experiments.[18,21] Scheme 1 shows the spin chemical

Scheme 1. Photocycle in Quinone-Blocked RCs of *Rb. sphaeroides* WT and R26[a]

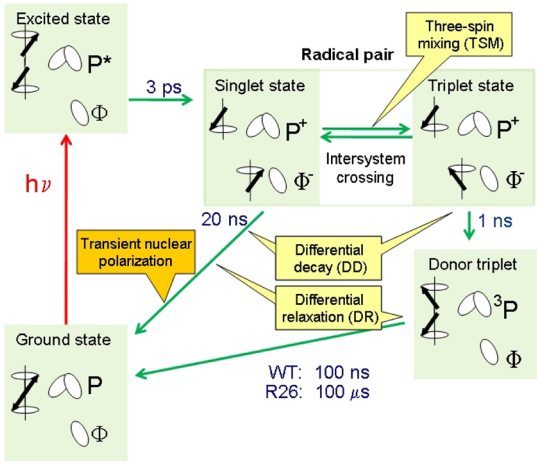

[a]Upon illumination and fast electron transfer from an excited singlet state, a radical pair is formed in a pure singlet state having high electron spin order. The radical pair is formed by a radical cation at the two donor BChls (special pair, P) and a radical anion on the BPhe acceptor cofactor (Φ) of the active branch. The chemical fate of the radical pair depends on its electronic spin state: while the singlet state is allowed to recombine, for the triplet state, a direct recombination is spin-forbidden and a donor triplet (^3P) is formed by intersystem crossing. Mechanisms building up photo-CIDNP under steady-state conditions are labeled in yellow. Transient nuclear polarization, which could be observed in time-resolved experiments, is labeled in orange.

cycle process that led to high nuclear polarization in RCs of *Rb. sphaeroides* WT and its carotenoid-less mutant R26. Under illumination with white light, the primary electron donor, which is a special pair of bacteriochlorophyll *a* (BChl *a*) molecules, is excited and forms a radical cation by donating an electron to the primary electron acceptor Φ, a bacteriopheophytin (BPhe). This leads to the formation of a spin-correlated radical pair, initially in its singlet state (S), which converts to the triplet state (T_0) by intersystem crossing (ISC). The high electron spin order of the initial pure electronic singlet state is transferred to a net nuclear polarization by two parallel mechanisms termed three-spin mixing (TSM)[22] and differential decay (DD).[23] The TSM mechanism is explained by anisotropic electron−electron dipolar coupling and pseudosecular hyperfine coupling (hfc), which breaks the symmetry of the spin-correlated radical pair. The polarization transfer by TSM occurs under the double matching condition where $2|\Delta\Omega| = 2|\omega_I| = |A|$, $\Delta\Omega$ is the difference in the electron Zeeman frequencies, ω_I is the nuclear Zeeman frequency, and A is the secular part of the hyperfine interaction. In the absence of anisotropic electron−electron dipolar coupling, the different lifetimes of the S and T_0 states cause polarization transfer by a DD mechanism. In the DD mechanism, the symmetry of the spin-correlated radical pair is broken by pseudosecular hyperfine coupling. The polarization

dx.doi.org/10.1021/bi300468y | *Biochemistry* 2012, 51, 5763−5773

transfer by the DD mechanism occurs due to a single matching condition of $2|\omega_I| = |A|$, and the difference between singlet and triplet radical pair lifetimes must be on the order of the inverse hfc. The emissive pattern of signals in the photo-CIDNP MAS NMR spectra of RCs of *Rb. sphaeroides* WT is due to these two competing mechanisms, and the relative intensity of these signals provides information about the spin density distribution of the radical pair.[19] In carotenoid-less mutant R26 of *Rb. sphaeroides* RCs that have a long-lived donor triplet, polarization transfer by a DR mechanism additionally occurs.[20,24] This is a modified radical pair mechanism (RPM) and depends on the different nuclear longitudinal relaxation rates.[18,25,26]

While electron polarization does not build up during subsequent photocycles, the long ^{13}C T_1 time[17] allows for the accumulation of nuclear polarization in a photo-CIDNP MAS NMR experiment. The effect has been shown to allow for a signal enhancement of >10000 and, hence, for the detection of cofactors directly in whole cells.[20,27] Recently, it has been demonstrated that the effect is not limited to frozen natural photosynthetic RCs at NMR fields; it also occurs in a blue-light photoreceptor,[28] in liquid membranes,[29] and is predicted to occur at earth's magnetic field.[30] Because the effect relies on hyperfine interactions, it requires a radical pair lifetime of at least tens of nanoseconds. Hence, any observation of the effect demonstrates that light-induced radical pairs having a lifetime significantly longer than 10 ns are present in a sample.

While the steady-state photo-CIDNP in RCs has been explained by the interplay of TSM, DD, and DR, in time-resolved experiments, transient nuclear polarization, occurring on the singlet decay channel only, can be detected (Scheme 1).[31] In R26 samples, the nuclear polarization originating from a singlet branch of the radical pair decays in 20 ns, while the decay of the nuclear polarization from the triplet state of the radical pair occurs in 100 μs. Therefore, transient nuclear polarization can be observed during the lifetime of the triplet donor.[21]

MATERIALS AND METHODS

Sample Preparation. Cells of *Hb. mobilis* strain ATCC 43427 (DSMZ 6151) were used in this study. The cells were cultured in medium no. 1552[32] anaerobically at 37 °C under continuous light. After growing for 7 days, cells were harvested by centrifugation (4000 rpm). One-half of the harvested cells were uniformly suspended in deoxygenated 20 mM Tris-HCl buffer (pH 8) containing 10 mM sodium ascorbate. Under a nitrogen gas flow, this sample (Braunstoff) was reduced with 50 mM sodium dithionite and packed in a 4 mm sapphire rotor for MAS NMR experiments. The other half of the harvested cells were used for preparing Grünstoff. These cells were washed with medium no. 1552 that does not contain sodium ascorbate. The cells were resuspended in the same non-ascorbate medium and were bubbled with oxygen gas under illumination. The conversion to Grünstoff was monitored by recording absorption spectra every 15 min. After 3 h, the conversion to Grünstoff was almost complete and the cells were collected by centrifugation. The cells were resuspended in 20 mM Tris-HCl buffer (pH 8) containing 10 mM sodium ascorbate and reduced with 50 mM sodium dithionite under a nitrogen gas flow. This sample (Grünstoff) was packed in a 4 mm sapphire rotor for MAS NMR experiments.

Because NH_4^+ ions seem to be the nitrogen source for the chlorophylls in *Hb. mobilis* cells,[8] $^{15}NH_4Cl$ was used as the precursor for ^{15}N labeling. The *Hb. mobilis* cells were grown anaerobically in medium no. 1552 that contained 46 mM $^{15}NH_4Cl$. The conversion to Grünstoff and the preparation of Braunstoff and Grünstoff samples for ^{15}N MAS NMR experiments were conducted as described above. For selective ^{13}C isotope labeling of BChls and Chls,[33] *Hb. mobilis* cells were grown anaerobically in medium no. 1552 containing 1 mM [4-^{13}C]-δ-aminolevulinic acid (ALA) or [3-^{13}C]ALA. C-1, C-3, C-6, C-8, C-11, C-13, C-17, and C-19 of BChls (Figure 2, red labels) were selectively isotope labeled by [4-^{13}C]ALA incorporation. The [3-^{13}C]ALA incorporation produces selective ^{13}C isotope labeling of C-2, C-3^1, C-7, C-8^1, C-12, C-13^1, C-17^1, and C-18 of BChls (Figure 2, blue labels). The conversion of Braunstoff to Grünstoff was conducted in both [4-^{13}C]ALA- and [3-^{13}C]ALA-labeled *Hb. mobilis* cells as described above. Both [4-^{13}C]- and [3-^{13}C]ALA-labeled Braunstoff and Grünstoff samples were reduced with 50 mM sodium dithionite and packed in 4 mm sapphire rotors for ^{13}C MAS NMR measurements.

MAS NMR Measurements. All ^{13}C and ^{15}N MAS NMR experiments in *Hb. mobilis* cells were conducted in a DMX 200 MHz spectrometer equipped with a 4 mm MAS probe (Bruker, Karlsruhe, Germany). The sample was packed into an optically transparent 4 mm MAS sapphire rotor and inserted into the MAS probe. A very low spinning frequency of 500 Hz was applied during freezing to achieve a homogeneous distribution of sample against the rotor wall.[34] The spinning frequency was increased to 8 kHz after the sample had been completely frozen at 235 K. For continuous illumination photo-CIDNP MAS NMR experiments, white light from a 1000 W xenon lamp was used. Both dark and photo-CIDNP spectra were obtained with a simple Hahn echo pulse sequence[35,36] with TPPM (two-pulse phase modulation) proton decoupling.[37] Laser flashes having pulse lengths of 6−8 ns and an energy of 20 mJ were used for time-resolved (TR) photo-CIDNP MAS experiments. The 532 nm laser flashes were produced using a Nd:YAG laser (Quanta-Ray INDI 40-10, SpectraPhysics, Irvine, CA). The same Hahn echo pulse sequence with TPPM proton decoupling was used for the TR photo-CIDNP MAS NMR experiment. Additional ^{13}C presaturation pulses were also used prior to a new experiment to extinguish the remaining coherence and polarization.[31] The nanosecond laser flash was synchronized with the 90° pulse of the Hahn echo pulse sequence using an external 500 MHz oscilloscope. The delay time Δ is the time between the nanosecond laser flash and the 90° NMR pulse. The ^{13}C and ^{15}N TR photo-CIDNP MAS experiments were performed on [^{15}N]- and [3-^{13}C]ALA-labeled *Hb. mobilis* cells by varying the delay time Δ.

In all NMR experiments, a recycle delay of 2 s was applied. ^{13}C MAS NMR signals of natural abundance and [^{13}C]ALA-labeled *Hb. mobilis* cells were collected for 40 and 12 h, respectively. ^{13}C TR experiments were conducted for 9 h in [3-^{13}C]ALA-labeled *Hb. mobilis* cells. Both dark and light ^{13}C MAS NMR spectra were referenced to the $^{13}COOH$ chemical shift of solid tyrosine-HCl at 172.1 ppm, and 50 Hz artificial line broadening was applied prior to Fourier transformation. All ^{15}N MAS NMR spectra were collected for 40 h. Chemical shifts are given relative to $^{15}NH_3$ using the response of solid $^{15}NH_4NO_3$ at δ 23.5 as a reference. For ^{15}N MAS NMR spectra, 20 Hz artificial line broadening was applied prior to Fourier transformation.

dx.doi.org/10.1021/bi300468y | *Biochemistry* 2012, 51, 5763−5773

RESULTS

^{15}N Photo-CIDNP MAS NMR Experiments. ^{15}N photo-CIDNP MAS NMR provides less complex data compared to the ^{13}C method, allowing for a more straightforward analysis.[38,39] Here we demonstrate that the solid-state photo-CIDNP effect can been observed with ^{15}N MAS NMR in whole cells of both forms of uniformly ^{15}N-labeled *Hb. mobilis* (Figure 3 and Figure S1 of the Supporting Information). In addition to the spectra of the two forms, the spectrum of a half-converted sample of *Hb. mobilis* cells is also shown (spectrum B in Figure 3). The respective ^{15}N MAS NMR spectra (A′−C′) measured under dark conditions are shown on the right side of Figure S1. In ^{15}N MAS spectra under dark conditions, only signals from the protein backbone are visible, while light-induced signals appear in the ^{15}N photo-CIDNP MAS NMR spectra. These light-induced ^{15}N MAS NMR signals of *Hb. mobilis* cells show emissive signs reminiscent of ^{15}N-labeled RCs of *Rb. sphaeroides*[15,40] and of PS II.[38] In Figure S1, both ^{15}N MAS NMR spectra under dark (A′) and light conditions (A) show a sharp signal at 23.5 ppm due to the presence of free NH_4^+ ions. During the conversion of *Hb. mobilis* cells to Grünstoff, the cells were resuspended in a medium that does not contain $^{15}NH_4Cl$. Therefore, the peak at 23.5 ppm is absent in spectra B and B′ and spectra C and C′.

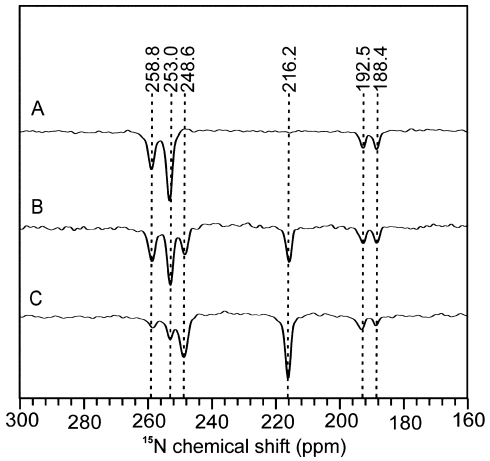

Figure 3. Expended view of ^{15}N photo-CIDNP MAS NMR spectra of anaerobically (Braunstoff) (A), half-converted (anaerobic/aerobic) (B), and aerobically treated (Grünstoff) (C) uniformly ^{15}N-labeled *Hb. mobilis* cells under illumination with continuous white light.

Figure 3 shows an expanded view of the ^{15}N photo-CIDNP MAS NMR spectra in Braunstoff (A) as well as that of half-converted (B) and Grünstoff (C) *Hb. mobilis* cells. In spectrum A, four signals appear at chemical shifts of 188.4, 192.5, 253.0, and 258.8 ppm. These signals were (Table S1 of the Supporting Information) preliminarily assigned by comparison to similar compounds such as Chl *a* in PS I and PS II[38] and BChl *a* of *Rb. sphaeroides* R26.[15,39] In BChl *g*, pyrrole ring II is different from that of Chl *a* and is similar to that of BChl *a*. It is clear from these assignments that all ^{15}N light-induced MAS NMR signals in the spectrum of Braunstoff are due to the four nitrogen atoms of BChl *g*′ of the donor while the signals from the acceptor are not present. The ^{15}N chemical shifts at 188.4, 258.8, 192.5, and 253.0 ppm are straightforwardly assigned to the N-I, N-II, N-III, and N-IV atoms of BChl *g*′, respectively. The primary donor in *Hb. mobilis* RCs was proposed to be a homodimer of BChl *g*′ molecules.[10] There is, in fact, no hint of doubling in the four signals. Because asymmetries as in the special pair induce chemical shift differences much larger than the line width of the peaks,[33] we conclude that the data presented in spectrum A of Figure 3 are in full agreement with the idea of an electronically highly symmetric homodimer.

In spectrum B, apart of these four signals from BChl *g*′, two signals with chemical shifts of 216.2 and 248.6 ppm appear and the intensities of the signals at 253.0 and 258.8 ppm decrease. The new signals at 216.2 and 248.6 ppm can be assigned to the N-II and N-IV atoms of the primary electron acceptor 8^1-OH Chl a_F (Table S1 of the Supporting Information). In spectrum C, the signals at 216.2 and 248.6 ppm (N-II and N-IV of 8^1-OH Chl a_F, respectively) have again higher intensities and the other signals at 253 and 258.8 ppm (N-II and N-IV of BChl *g*′, respectively) decrease further in intensity. The two ^{15}N NMR signals at 188.4 and 192.5 ppm (N-I and N-III, respectively) remain unchanged during the conversion, implying that the chemical shifts are similar in both BChl *g*′ and 8^1-OH Chl a_F cofactors. The mixed sample (spectrum B) does not show any additional signal that would not belong to Braunstoff or Grünstoff. That suggests that the transformation does not lead to stable asymmetric states in which one-half of the RC is transformed and the other is not.

From the analysis described above, it is evident that in both forms, Braunstoff and Grünstoff, radical pairs are present on the time scale of at least tens of nanoseconds. It appears that the chemical composition of the donor remains unchanged. Hence, the color change is not caused by a change in the donor cofactors. Also because the acceptor signals in Grünstoff are not split, it appears that the strongly symmetric character remains intact upon transformation.

Assuming that the photo-CIDNP intensities of steady-state experiments correlate with electron spin densities in p orbitals,[38] we find that Braunstoff shows similarities to PS II, having its highest electron spin density in the N-IV atoms of pyrrole ring IV.[38] On the other hand, the highest electron spin density of Grünstoff is observed on the N-II atoms, and this is similar to the case for PS I.[38]

^{13}C Photo-CIDNP MAS NMR on Natural Abundance Samples. Here we demonstrate that the solid-state photo-CIDNP effect is also observed in both natural abundance (n.a.) Braunstoff and Grünstoff *Hb. mobilis* cells by ^{13}C MAS NMR. In spectra A and C of Figure 4, the samples are measured in the dark and only weak and broad features from the protein are visible. Spectra B and D are the ^{13}C photo-CIDNP spectra of Braunstoff and Grünstoff, respectively, obtained under continuous illumination. Several light-induced signals are observed in the region between 200 and 80 ppm. The ^{13}C photo-CIDNP spectrum of Braunstoff shows emissive (negative) and absorptive (positive) light-induced signals comparable to those of RCs from *Rb. sphaeroides* R26[20] and PS II.[41] The pattern suggests the occurrence of the DR mechanism, implying a long-lived donor triplet state (^{3}P) and the absence of carotenoids close to the donor. Upon conversion, all the photo-CIDNP signals exhibit emissive patterns even though the chemical shifts of the signals are almost the same as the signals in Braunstoff (Figure 5).

Figure 5 shows an expanded view of the aromatic region of the ^{13}C photo-CIDNP MAS NMR spectra of n.a. Braunstoff and Grünstoff cells. The chemical shifts from Braunstoff (parallel to the green bar) and Grünstoff (parallel to the red bar) are compared with the chemical shifts of Chl *a* and BChl *a*

dx.doi.org/10.1021/bi300468y | *Biochemistry* 2012, 51, 5763−5773

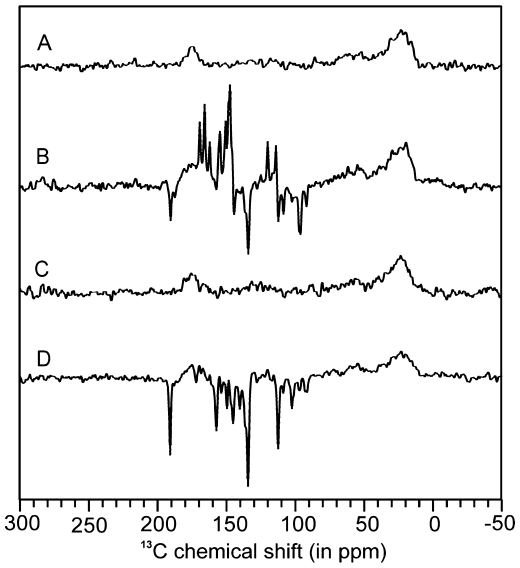

Figure 4. ^{13}C MAS NMR spectra of *Hb. mobilis* cells. The dark spectrum (A) and the spectrum under illumination (B) of Braunstoff. The dark spectrum (C) and spectrum under illumination (D) of Grünstoff. The spectra were obtained at 4.7 T and 235 K within 40 h from whole cells at natural abundance. For illumination, white light from a xenon lamp was used. Prior to illumination, the heliobacterial cells were reduced with sodium dithionite.

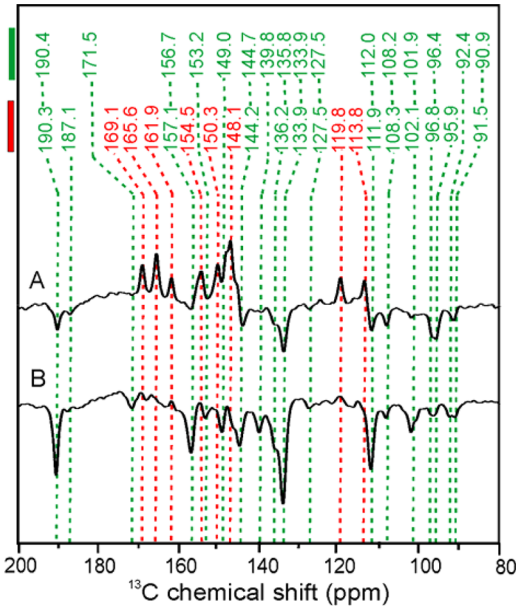

Figure 5. Aromatic part of the ^{13}C photo-CIDNP MAS NMR spectra of anaerobically (Braunstoff) (A) and aerobically (Grünstoff) (B) treated *Hb. mobilis* cells. Chemical shift values denoted parallel to the red bar belong to Braunstoff, and the assignments parallel to the green bar belong to Grünstoff. Red lines are absorptive peaks and green lines emissive peaks.

obtained from other photo-CIDNP studies (Table S2 of the Supporting Information). It is evident that the positive signals disappear while the intensities of the negative signals increase. Because the identity of the cofactors is not changed, we assume that their interaction is modified, leading to different activities of the three competing mechanisms. The negative signal at 190.3 ppm can be assigned to the C-13^1 carbonyl atom of the acceptor 8^1-OH Chl a_F. The positive signals at 169.1, 165.6, 161.9, 154.5 150.3, 148.1, 119.8, and 113.8 ppm, which are absent in the spectra of Grünstoff, can be straightforwardly assigned to C-6, C-19, C-14, C-1, C-16, C-4, C-12, and C-3^1, respectively, of the donor BChl *g*′. The negative signals at 171.5, 157.1, 153.2, 149.0, 144.7, 139.8, 133.9, and 112 ppm match well to C-6, C-1, C-16, C-9, C-8, C-3, and C-3^2 atoms of acceptor 8^1-OH Chl a_F. Hence, we conclude from the chemical shift patterns that in Braunstoff all the light-induced absorptive signals are due to BChl *g*′ (the electron donor) and in both forms the emissive signals are due to 8^1-OH Chl a_F (the electron acceptor).

The signals in the region of methine carbons show an emissive pattern in both Braunstoff and Grünstoff (for an expanded view, see Figure S2 of the Supporting Information). The signals at 108.3 and 102.1 ppm correspond to C-10 and C-15 of 8^1-OH Chl a_F, respectively. The methine C-5 atom is observed as a doublet (96.8 and 95.9 ppm) in Braunstoff, while in Grünstoff, only a single signal (96.4 ppm) occurs. On the other hand, the methine C-20 atom in Grünstoff is split (92.4 and 90.9 ppm) but not in Braunstoff (91.5 ppm). Assuming that in both cases the negative signals originate from the acceptor, the splitting implies that in both forms two acceptors are active, which are slightly distinguishable and are probably the two acceptor 8^1-OH Chl a_F molecules. That would imply that both branches of cofactors are active, similar to the case proposed for PS I.[42]

From the constancy of the chemical shifts in all regions, we conclude that in both forms the spin-correlated radical pair is formed by the identical set of cofactors. This would imply that the color change is not caused by the cofactors forming the radical pair but by cofactors in the environment of those forming the radical pair. Because the intensity pattern is dramatically affected, one might conclude that the accessory cofactors are also affected, leading to altered interactions within the radical pair.

^{13}C Photo-CIDNP MAS NMR on Selectively ^{13}C-Labeled Samples. Selective enhancement of ^{13}C photo-CIDNP MAS NMR signals in the spectra described above can assist in the assignment of the light-induced signals. ^{13}C isotope labeling of the cofactors has been achieved (Figure 2) in the RCs of Braunstoff and Grünstoff by applying selectively labeled aminolevulinic acid (ALA) as precursor. The position of the ^{13}C label in the RC cofactors depends on the position of the ^{13}C label in the precursor ALA. Both [4-^{13}C]ALA and [3-^{13}C]ALA precursors have been used in this study.

^{13}C photo-CIDNP MAS NMR spectra of [4-^{13}C]ALA-labeled *Hb. mobilis* cells are shown in Figure S3 of the Supporting Information. Spectra A and B originate from Braunstoff and Grünstoff, respectively. Apart from the signals in the aromatic region, one light-induced signal is observed in the aliphatic region in both spectra. It originates from C-17 of the donor, which gains signal intensity via ^{13}C−^{13}C spin diffusion from the nearby aromatic carbons of the cofactor.[21] In the spectrum of Braunstoff, only absorptive signals are strongly enhanced. In the spectrum of Grünstoff, both strongly enhanced positive and negative signals are observed. A shift in intensity from negative to positive signals upon isotope labeling is evident and demonstrates that magnetic nuclei actively participate in the spin dynamical process. Interestingly, in the 3-ALA-labeled sample (vide infra), in which the magnetic isotopes are more distant from the π-system, the shift in the intensity is less pronounced. A theoretical description of multilabeling effects is challenging and will be treated in a later

dx.doi.org/10.1021/bi300468y | *Biochemistry* 2012, 51, 5763−5773

study. Because isotope labeling modifies the photo-CIDNP intensities, the concentration of the isotope label is difficult to extract by comparing signals from labeled and unlabeled positions. However, we were not able to observe cross-peaks in two-dimensional experiments, suggesting that the level of label incorporation is <50%.

The expanded view of the light-induced signals from [4-^{13}C]ALA-labeled *Hb. mobilis* cells in both forms is presented in Figure 6. The absorptive light-induced signals at chemical

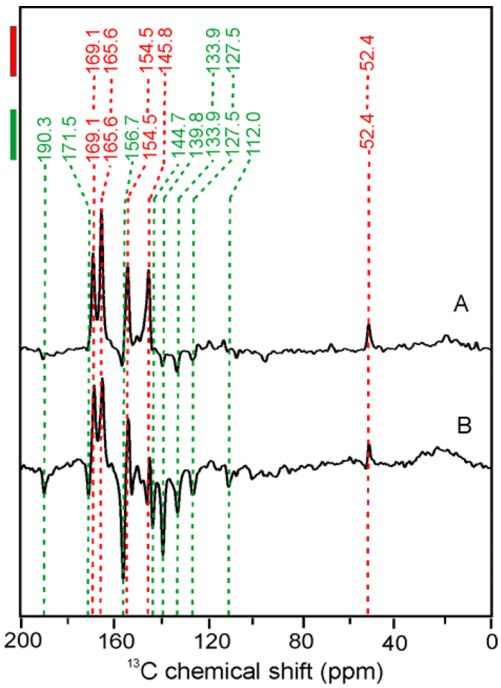

Figure 6. Expanded view of the ^{13}C photo-CIDNP MAS NMR spectra of anaerobically (Braunstoff) (A) and aerobically (Grünstoff) (B) treated 4-ALA-labeled *Hb. mobilis* cells. Chemical shift values parallel to the red bar belong to Braunstoff, and the assignments parallel to the green bar belong to Grünstoff. Red lines are absorptive peaks and green lines emissive peaks.

shifts of 165.6, 154.5, 169.1, and 145.8 ppm correspond to C-19, C-1, C-6, and C-11 of the donor BChl *g*′ (see the red labels in Figure 2A) in both Braunstoff and Grünstoff. The absorptive signal in the aliphatic region at 52.4 ppm belongs to C-17 of BChl *g*′, which is the only aliphatic ^{13}C-labeled carbon using [4-^{13}C]ALA labeling. The emissive light-induced signals at chemical shifts of 156.7. 171.5, 144.7, 139.8, and 127.5 ppm correspond to C-1, C-6, C-8, C-3, and C-13, respectively, of the primary acceptor 8^1-OH Chl a_F (see the red labels in Figure 2B). Again, it is evident that the chemical shifts of the donor and acceptor are not doubled and are not changed upon conversion, demonstrating that the functional symmetry and identity of the active cofactors are not affected.

^{13}C photo-CIDNP MAS NMR spectra of [3-^{13}C]ALA-labeled *Hb. mobilis* cells are also observed (Figure 7 and Figure S4 of the Supporting Information) for both Braunstoff (A) and Grünstoff (B). The spectrum of Braunstoff shows mixed patterns of absorptive and emissive light-induced signals. The fact that the signal intensity of the positive signal in the aliphatic region (43.5 ppm, C-7 of the donor) is stronger than that of labeled aromatic carbons might be due to local dynamics. The positive signals in the aliphatic region are due to

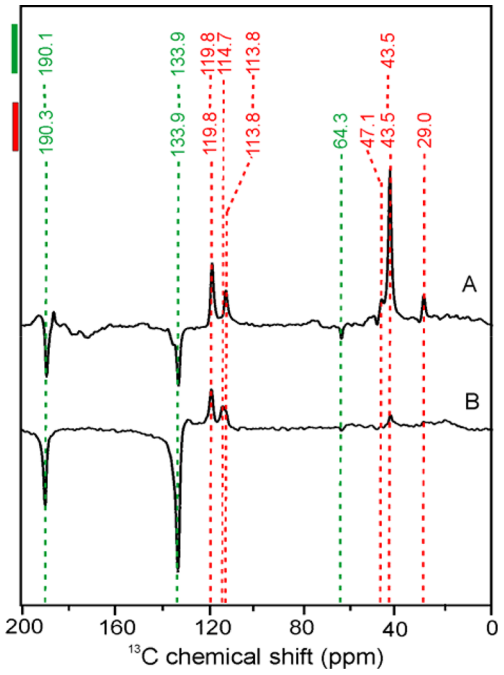

Figure 7. Expanded view of the ^{13}C photo-CIDNP MAS NMR spectra of anaerobically (Braunstoff) (A) and aerobically (Grünstoff) (B) treated 3-ALA-labeled *Hb. mobilis* cells. Chemical shift values parallel to the red bar belong to Braunstoff, and the assignments parallel to the green bar belong to Grünstoff. Red lines are absorptive peaks and green lines emissive peaks.

C-7, C-17^1, and C-18 of the primary donor BChl *g*′ (see the blue labels in Figure 2A). The isolated signal at 29.0 ppm originates from C-17^1 of the donor, while the only emissive signal in the aliphatic region occurs at 64.3 ppm and can be straightforwardly assigned to C-8^1 of the acceptor (Figure 2B). The small negative signals near the 29 and 47 ppm signals belong to C-17^1 and C-18, respectively, of the primary acceptor 8^1-OH Chl a_F. Hence, the isotope labeling experiment supports the assignment of the positive signals to the donor cofactor and of the negative signals to the acceptor cofactor.

The absorptive signals at 119.8 and 113.8 ppm in the aromatic region correspond to C-12 and C-13 of BChl *g*′, respectively. The emissive light-induced signals at 190.3 and 133.9 ppm correspond to C-13^1 and C-2 of the acceptor 8^1-OH Chl a_F, respectively. These are the most intense signals in the spectrum of Grünstoff. Table S2 of the Supporting Information summarizes the assignments. There is one absorptive signal originating from C-3^1 of the BChl *g*′ donor in the spectrum of Grünstoff that appears to be doubled (113.8 and 114.7 ppm). Because C-3^1 belongs to the overlap region of two BChl *g*′ cofactors, one might assume that the doubling of the signal is an indication of a slight perturbation of one of the two cofactors in the dimeric donor. That would imply that the donor is indeed dimeric and a special pair type.

In both spectra, positive and negative signals appear to be very sharp, having almost equal line widths of 35 Hz. The observation of very sharp lines from the cofactors seems to be a general feature of RCs,[33,34,38] providing a well-defined, well-ordered, and solid structure without protein disorder. These features remain intact upon photoconversion to Grünstoff.

Time-Resolved (TR) Photo-CIDNP MAS NMR Experiments. TR photo-CIDNP MAS NMR experiments allow for observation of the evolution of spin dynamics and of the

dx.doi.org/10.1021/bi300468y | *Biochemistry* 2012, 51, 5763−5773

reaction kinetics of the radical pair on a microsecond time scale.[21,31] Here we report TR data obtained from both Braunstoff and Grünstoff in solid-state photo-CIDNP MAS NMR experiments on uniformly ^{15}N-labeled and [3-^{13}C]ALA-labeled *Hb. mobilis* cells using nanosecond laser flashes. The time resolution was obtained by varying the delay time Δ, which is the time difference between the laser pulse and the beginning of the NMR $\pi/2$ detection pulse.

Figure 8 shows the photo-CIDNP ^{15}N MAS NMR spectra of *Hb. mobilis* cells (Braunstoff). The top spectrum (A) is the

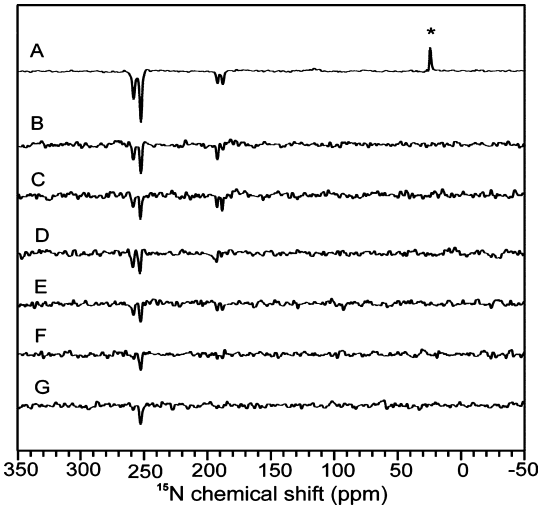

Figure 8. Series of time-resolved ^{15}N photo-CIDNP spectra of uniformly ^{15}N labeled *Hb. mobilis* cells, anaerobically treated (Braunstoff). The spectra were obtained at a magnetic field of 4.7 T and a temperature of 235 K. The laser pulses have a length of ∼10 ns and a wavelength of 532 nm. The delay time between the laser pulse and NMR measurement was 0 (B), 10 (C), 30 (D), 50 (E), 100 (F), or 200 μs (G). The spectrum at the top (A), obtained under continuous illumination, is shown for comparison.

photo-CIDNP MAS NMR spectrum under continuous illumination (C.I.) with white light. The following are the TR photo-CIDNP MAS NMR spectra obtained by varying the delay time from 0 (B) to 200 μs (G). In the Δ = 0 μs spectrum (B), four signals at chemical shifts of 188.4, 258.8, 193.1, and 253.0 ppm occur, corresponding to the N-I, N-II, N-III, and N-IV atoms of BChl *g*′, respectively (see above). The spectra were collected with delay times of 10 (C), 30 (D), 50 (E), 100 (F), and 200 μs (G). Compared to the spectrum obtained under C.I., these TR spectra show a lower signal-to-noise ratio. The intensity of light-induced signals decays with an increase in the delay time from 0 to 100 μs, especially for the signals at chemical shifts of 188.4 (N-I) and 193.1 ppm (N-III). The light-induced signal at 253 ppm persists at the delay time of 200 μs and beyond. A very similar pattern of decay of light-induced signals with an increase in the delay time was observed in TR photo-CIDNP MAS NMR measurements of *Rb. sphaereoides* R26.[39] In that case, the decay was explained as the lifetime of the donor triplet state (^{3}P), during which solely the nuclear polarization decaying on the singlet decay branch can be observed. In the time evolution of Braunstoff, the same kinetics is found in the parallel decay of three signals at that time scale, while steady-state nuclear polarization is built up, leading to the dominant signal at 253.0 ppm. This would imply that in Braunstoff, the absence of a nearby carotenoid leads to a long-lived ^{3}P state. From Grünstoff, probably because of insufficient labeling, we were not able to obtain TR photo-CIDNP ^{15}N MAS NMR data.

From [3-^{13}C]ALA-labeled *Hb. mobilis* cells, high-quality TR photo-CIDNP spectra have been obtained. The set of TR photo-CIDNP spectra of Braunstoff with different delay times (Δ) is shown in Figure 9. The spectrum with a delay time of 0

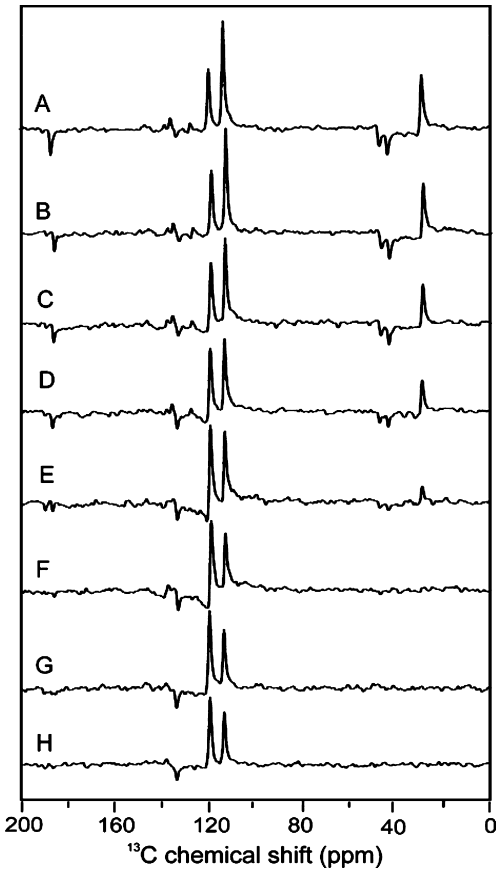

Figure 9. Series of time-resolved ^{13}C photo-CIDNP MAS NMR spectra of 4-ALA-labeled *Hb. mobilis* cells, anaerobically (Braunstoff) treated. The spectra were obtained at a magnetic field of 4.7 T and a temperature of 235 K. The laser pulses have a length of ∼10 ns and a wavelength of 532 nm. The delay time between the laser pulse and NMR measurement was 0 μs (A), 10 μs (B), 30 μs (C), 50 μs (D), 100 μs (E), 200 μs (F), 500 μs (G), or 1 ms (H).

μs (A) shows the light-induced signals are almost similar to the steady-state photo-CIDNP MAS NMR spectra of [3-^{13}C]ALA-labeled Braunstoff (see Figure 7A) except for the absence of the emissive signal at 133.9 ppm, the occurrence of the signal at 187.0 ppm, and the different phasing of the signals in the aliphatic region. The aliphatic signal disappears within ∼100 μs, demonstrating the presence of transient nuclear polarization on this time scale.[21] In the same period, also the transient signal of the carbonyl carbon at 187.0 ppm disappears and the emissive signal at 133.9 ppm evolves. After 100 μs, the light-induced signals are caused by the steady-state photo-CIDNP effect. Hence, the time evolution clearly demonstrates that the transient nuclear polarization of the singlet channel decays after 100 μs, which matches the period known from *Rb. sphaeroides* R26.[21] This demonstrates the presence of a long-lived donor triplet state (^{3}P) in Braunstoff.

Figure 10 shows a set of TR photo-CIDNP ^{13}C MAS NMR spectra of [3-^{13}C]ALA-labeled cells of Grünstoff. It appears that

dx.doi.org/10.1021/bi300468y | *Biochemistry* 2012, 51, 5763−5773

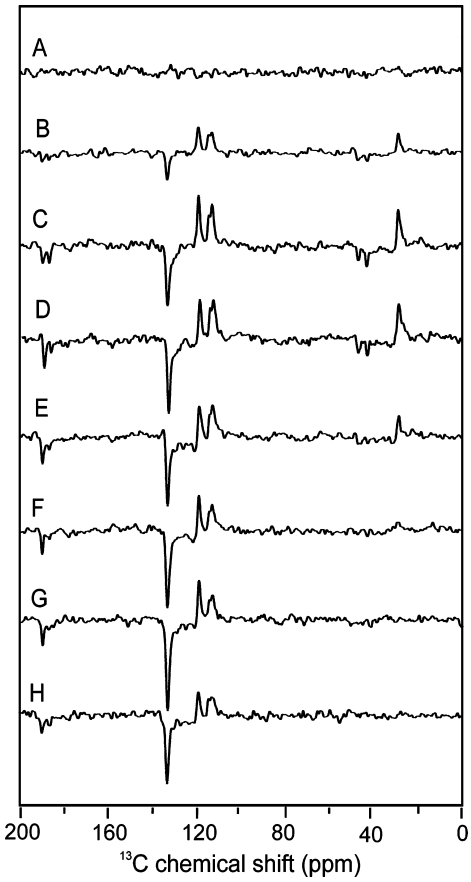

Figure 10. Series of time-resolved ^{13}C photo-CIDNP MAS NMR spectra of 4-ALA-labeled *Hb. mobilis* cells, aerobically (Grünstoff) treated. The spectra were obtained at a magnetic field of 4.7 T and a temperature of 235 K. The laser pulses have a length of ~10 ns and a wavelength of 532 nm. The delay time between the laser pulse and NMR measurement was 0 μs (A), 10 μs (B), 30 μs (C), 50 μs (D), 100 μs (E), 200 μs (F), 500 μs (G), or 1 ms (H).

the kinetics of the decay of transient nuclear polarization is similar to that observed in Braunstoff because the transient features disappear on a time scale of 100 μs. The similarity of the spectral features of the transient nuclear polarization and the conservation of its decay kinetics again demonstrate that the identity of the cofactors forming the radical pair is not changed upon phototransformation. There is, however, a remarkable difference in the time evolution of both forms. Unlike the TR spectrum of Braunstoff, there are no light-induced signals observed in the TR spectrum of Grünstoff in the initial 10 μs (Figure 10 and Figure S5 of the Supporting Information). Such a "silent" initial period has not yet been reported in other RCs.

DISCUSSION

Structure of the Primary Radical Pair in Braunstoff. There are several lines of evidence that show that the overall radical pair kinetics is very similar to those in RCs of *Rb. sphaeroides* R26 and contrasts with those of *Rb. sphaeroides* WT. The positive sign of the donor signals, the proposed occurrence of the DR mechanism, and in particular the triplet kinetics match very well with the data from R26 RCs. These striking similarities imply a similar overall cofactor arrangement with a central special pair, accessory cofactors, and primary acceptor cofactors, all of which lead to similar dynamics of electron transfer, spin dynamics, and triplet lifetimes. The latter provides evidence of the absence of nearby triplet quenchers as carotenoids. Hence, the primary radical pair of Braunstoff consists of a dimer of BChl g' molecules as electron donors and two 8^1-OH Chl a_F cofactors as primary electron acceptors. We also conclude that the ^3P state is, we assume symmetrically, spread over both donor cofactors.

Any difference with the heterodimeric R26 RCs is due to the homodimeric symmetry of the RC subunits in heliobacteria. Indeed, there is no indication of signal doubling at the donor site, which is best interpreted as an absolutely symmetrically arranged dimer. At the acceptor site, we observe doubling for a single signal that occurs in the methylene carbon region. In that region, five instead of four signals are present; obviously, those at 96.8 and 95.9 ppm (Figure S2 of the Supporting Information), having the same intensity, are both assigned to C-5 of an 8^1-OH Chl a_F cofactor. Hence, at the acceptor side, a very minor difference occurs, implying that both branches are equally active. The functional activity on both branches of electron transfer cofactors has also been demonstrated for PS I.[42,43]

Structure of the Early Radical Pair in Grünstoff. We put forward several arguments that the cofactors that form the radical pair in the NMR experiments are chemically unchanged. In particular, the chemical shift patterns of absorptive and emissive signals remain almost identical between Braunstoff and Grünstoff. In addition, the kinetics of the decay of the donor triplet does not change, suggesting that the localization of the donor triplet is identical, and most likely also the special pair donor. Also in Grünstoff, both branches appear to be active as shown by the slight doubling of the signals at 92.4 and 90.6 ppm (C-20) and 101.9 and 100.4 ppm (C-15) (Figure S2 of the Supporting Information). There might be a slight asymmetry of intensities that can be observed at the C-5 signal of the acceptor at ~96.4 ppm. The fact that the functional symmetry remains upon phototransformation demonstrates that the general radical pair structure remains unchanged and is robust. In particular, we conclude that the phototransformation acts symmetrically on both parts of the homodimer.

There are two significant differences between the spectra of Braunstoff and Grünstoff. (i) The ratio between absorptive and emissive signals is shifted. This is certainly due to the weakening of the effect of DR in the first 10 μs as demonstrated in the time-resolved experiments. In addition, it might indicate a difference in the composition of the contributions of the solid-state photo-CIDNP mechanisms in favor of TSM. Because the cofactors that form the radical pair remain unchanged, one might conclude that the accessory cofactors bridging the radical cation and radical anion become modified. Such a modification would directly affect the electron−electron coupling and lead to a change in the ratio between contributions from TSM and DD. (ii) The silent initial phase occurs during the triplet evolution of Grünstoff. Assuming that between 10 and 100 μs the donor triplet state is localized on the special pair, it appears it is preceded by early mobility of either the radical cation or the donor triplet state. Because the radical cation decays on the nanosecond time scale, the observed dynamics is due to the donor triplet. We therefore assume that the donor triplet is mobile and formed on another cofactor, most likely a photoconverted accessory cofactor, before it migrates after 10 μs onto the special pair.

Functional Flexibility. Because the cofactors that form the radical pair are identical but their coupling is not, we propose

dx.doi.org/10.1021/bi300468y | *Biochemistry* 2012, 51, 5763−5773

that the accessory cofactor is modified by the photo-transformation from BChl *g* to Chl a_F. The newly formed Chl a_F also carries the donor triplet state, which moves after 10 μs to the special pair. The presence of donor triplet state on accessory chlorophylls has been reported in PS II at cryogenic temperatures.[44,45] In both plant RCs, an accessory pigment also acts as the primary electron donor,[46−49] although on an NMR time scale the stabilized radical pair is observed.[38,50] Similarly, charge separation in RCs of *Rb. sphaeroides* that occurs with the participation of accessory pigments[51] is observed on the time scale of an NMR experiment as a radical cation of the special pair. Here we would like to stress that the radical pair observed in Grünstoff might not be the primary radical pair, but a product of a stabilization process on the submicrosecond time scale.

The RCs of heliobacteria have been proposed to be ancestors of PS I. On one hand, bidirectional electron transfer is a feature of PS I. On the other hand, the possible involvement of an accessory cofactor in triplet formation is reminiscent of PS II, although heliobacterial RCs do not appear to be an evolutionary ancestor of the latter. This would imply that the function of RCs is rather flexible. RCs maintain a general cofactor architecture, which can be homodimeric, which is functionally robust for changes in the matrix, and which simply leads to changes of the pathways but not a change in function. Hence, the transformation of heliobacteria confirms the remarkable combination of the robustness, efficiency, and flexibility of natural RCs.

■ ASSOCIATED CONTENT

Supporting Information

Light and dark spectra of ^{15}N-labeled *Hb. mobilis* cells of Braunstoff, half-converted to Grünstoff, and Grünstoff; assignments of ^{15}N photo-CIDNP MAS NMR signals; methylidine region of the ^{13}C photo-CIDNP MAS spectra of unlabeled *Hb. mobilis* cells of Braunstoff and Grünstoff; ^{13}C photo-CIDNP MAS spectra of [4-^{13}C]ALA- and [3-^{13}C]ALA-labeled *Hb. mobilis* cells of Braunstoff and Grünstoff; assignments of ^{13}C photo-CIDNP MAS NMR signals; and series of TR ^{13}C photo-CIDNP MAS spectra of [3-^{13}C]ALA-labeled *Hb. mobilis* cells of Grünstoff with Δ values of 0−50 μs. This material is available free of charge via the Internet at http://pubs.acs.org.

■ AUTHOR INFORMATION

Corresponding Author

*J.H.G.: phone, (814) 865 1163; e-mail, jhg5@psu.edu. J.M.: phone, +31-71-5274198; e-mail, j.matysik@chem.leidenuniv.nl.

Present Address

[§]Department of Chemistry, Brandeis University, Waltham, MA 02454-9110, and Francis Bitter Magnet Laboratory, Massachusetts Institute of Technology, Cambridge, MA 02139-4307.

Funding

This work was supported by The Netherlands Organization for Scientific Research (NWO) through a Middelgroot Grant (700.57.107) to J.M. and the Division of Chemical Sciences, Geosciences, and Biosciences, Office of Basic Energy Sciences of the U.S. Department of Energy, via Grant DE-FG02-08ER15989 to J.H.G.

Notes

The authors declare no competing financial interest.

■ ACKNOWLEDGMENTS

We thank A. H. M. de Wit for his help in culturing the bacteria. Helpful discussions with Prof. G. Jeschke and G. J. Janssen are acknowledged. F. Lefeber, K. B. Sai Sankar Gupta, K. Erkelens, and Bryan Ferlez are gratefully acknowledged.

■ ABBREVIATIONS

ALA, aminolevulinic acid; BChl, bacteriochlorophyll; BPhe, bacteriopheophytin; Chl, chlorophyll; Chl a_F, chlorophyll *a* with a farnesyl side chain; C.I., continuous illumination; DD, differential decay; DR, differential relaxation; EPR, electron paramagnetic resonance; FT-IR, Fourier transform infrared spectroscopy; ISC, intersystem crossing; MAS, magic angle spinning; NMR, nuclear magnetic resonance; P, special pair primary electron donor; photo-CIDNP, photochemically induced dynamic nuclear polarization; PS I, photosystem I; PS II, photosystem II; RC, reaction center; RPM, radical pair mechanism; S, singlet; T_0, triplet; TPPM, two-pulse phase modulation; TR, time-resolved; TSM, electron−electron nuclear three-spin mixing; WT, wild type.

■ REFERENCES

(1) Gest, H. (1994) Discovery of the heliobacteria. *Photosynth. Res. 41*, 17−21.

(2) Stevenson, A. K., Kimble, L. K., Woese, C. R., and Madigan, M. T. (1997) Characterization of new phototrophic heliobacteria and their habitats. *Photosynth. Res. 53*, 1−11.

(3) Golbeck, J. (2007) The heliobacterial reaction center. *Photosynth. Res. 91*, 139−140.

(4) Vassiliev, I. R., Antonkine, M. L., and Golbeck, J. H. (2001) Iron-sulfur clusters in type I reaction centers. *Biochim. Biophys. Acta 1507*, 139−160.

(5) Nitschke, W., and Rutherford, A. W. (1991) Photosynthetic reaction centers: Variations on a common structural theme. *Trends Biochem. Sci. 16*, 241−245.

(6) Liebl, U., Mockensturmwilson, M., Trost, J. T., Brune, D. C., Blankenship, R. E., and Vermaas, W. (1993) Single core polypeptide in the reaction center of the photosynthetic bacterium *Heliobacillus mobilis*: Structural implications and relations to other photosystems. *Proc. Natl. Acad. Sci. U.S.A. 90*, 7124−7128.

(7) Olson, J. M., and Blankenship, R. E. (2004) Thinking about the evolution of photosynthesis. *Photosynth. Res. 80*, 373−386.

(8) Gest, H., and Favinger, J. L. (1983) *Heliobacterium chlorum*, an anoxygenic brownish green photosynthetic bacterium containing a new form of bacteriochlorophyll. *Arch. Microbiol. 136*, 11−16.

(9) Brockmann, H., and Lipinski, A. (1983) Bacteriochlorophyll *g*, a new bacteriochlorophyll from *Heliobacterium chlorum*. *Arch. Microbiol. 136*, 17−19.

(10) Kobayashi, M., van de Meent, E. J., Erkelens, C., Amesz, J., Ikegami, I., and Watanabe, T. (1991) Bacteriochlorophyll g epimer as a possible reaction center component of heliobacteria. *Biochim. Biophys. Acta 1057*, 89−96.

(11) van de Meent, E. J., Kobayashi, M., Erkelens, C., van Veelen, P. A., Amesz, J., and Watanabe, T. (1991) Identification of 8^1-hydroxychlorophyll a as a functional reaction center pigment in heliobacteria. *Biochim. Biophys. Acta 1058*, 356−362.

(12) Nabedryk, E., Leibl, W., and Breton, J. (1996) FTIR spectroscopy of primary donor photooxidation in photosystem I, *Heliobacillus mobilis*, and *Chlorobium limicola*. Comparison with purple bacteria. *Photosynth. Res. 48*, 301−308.

(13) Prince, R. C., Gest, H., and Blankenship, R. E. (1985) Thermodynamic properties of the photochemical reaction center of *Heliobacterium chlorum*. *Biochim. Biophys. Acta 810*, 377−384.

(14) Roy, E., Rohmer, T., Gast, P., Jeschke, G., Alia, A., and Matysik, J. (2008) Characterization of the primary radical pair in reaction

centers of *Heliobacillus mobilis* by ^{13}C photo-CIDNP MAS NMR. *Biochemistry 47*, 4629−4635.
(15) Zysmilich, M. G., and McDermott, A. (1994) Photochemically induced dynamic nuclear-polarization in the solid-state N-15 spectra of reaction centers from photosynthetic bacteria *Rhodobacter sphaeroides* R-26. *J. Am. Chem. Soc. 116*, 8362−8363.
(16) Matysik, J., Diller, A., Roy, E., and Alia, A. (2009) The solid-state photo-CIDNP effect. *Photosynth. Res. 102*, 427−435.
(17) Daviso, E., Jeschke, G., and Matysik, J. (2008) Photochemically induced dynamic nuclear polarization (photo-CIDNP) magic-angle spinning NMR. In *Biophysical Techniques in Photosynthesis II* (Aartsma, T., and Matysik, J., Eds.) pp 385−399, Springer, Dordrecht, The Netherlands.
(18) Jeschke, G., and Matysik, J. (2003) A reassessment of the origin of photochemically induced dynamic nuclear polarization effects in solids. *Chem. Phys. 294*, 239−255.
(19) Prakash, S., Alia, Gast, P., de Groot, H. J. M., Jeschke, G., and Matysik, J. (2005) Magnetic field dependence of photo-CIDNP MAS NMR on photosynthetic reaction centers of *Rhodobacter sphaeroides* WT. *J. Am. Chem. Soc. 127*, 14290−14298.
(20) Prakash, S., Alia, Gast, P., de Groot, H. J. M., Matysik, J., and Jeschke, G. (2006) Photo-CIDNP MAS NMR in intact cells of *Rhodobacter sphaeroides* R26: Molecular and atomic resolution at nanomolar concentration. *J. Am. Chem. Soc. 128*, 12794−12799.
(21) Daviso, E., Alia, A., Prakash, S., Diller, A., Gast, P., Lugtenburg, J., Matysik, J., and Jeschke, G. (2009) Electron-nuclear spin dynamics in a bacterial photosynthetic reaction center. *J. Phys. Chem. C 113*, 10269−10278.
(22) Jeschke, G. (1997) Electron-electron-nuclear three-spin mixing in spin-correlated radical pairs. *J. Chem. Phys. 106*, 10072−10086.
(23) Polenova, T., and McDermott, A. E. (1999) A coherent mixing mechanism explains the photoinduced nuclear polarization in photosynthetic reaction centers. *J. Phys. Chem. B 103*, 535−548.
(24) McDermott, A., Zysmilich, M. G., and Polenova, T. (1998) Solid state NMR studies of photoinduced polarization in photosynthetic reaction centers: Mechanism and simulations. *Solid State Nucl. Magn. Reson. 11*, 21−47.
(25) Goldstein, R. A., and Boxer, S. G. (1987) Effects of nuclear-spin polarization on reaction dynamics in photosynthetic bacterial reaction centers. *Biophys. J. 51*, 937−946.
(26) Closs, G. L. (1975) Overhauser mechanism of chemically-induced nuclear-polarization as suggested by Adrian. *Chem. Phys. Lett. 32*, 277−278.
(27) Janssen, G. J., Daviso, E., van Son, M., de Groot, H. J. M., Alia, A., and Matysik, J. (2010) Observation of the solid-state photo-CIDNP effect in entire cells of cyanobacteria *Synechocystis*. *Photosynth. Res. 104*, 275−282.
(28) Thamarath, S. S., Heberle, J., Hore, P. J., Kottke, T., and Matysik, J. (2010) Solid-state photo-CIDNP effect observed in Phototropin LOV1-C57S by ^{13}C magic-angle spinning NMR spectroscopy. *J. Am. Chem. Soc. 132*, 15542−15543.
(29) Daviso, E., Janssen, G. J., Alia, A., Jeschke, G., Matysik, J., and Tessari, M. (2011) A 10000-fold nuclear hyperpolarization of a membrane protein in the liquid phase via solid-state mechanism. *J. Am. Chem. Soc. 133*, 16754−16757.
(30) Jeschke, G., Anger, B. C., Bode, B. E., and Matysik, J. (2011) Theory of solid-state photo-CIDNP in the earth's magnetic field. *J. Phys. Chem. A 115*, 9919−9928.
(31) Daviso, E., Diller, A., Alia, A., Matysik, J., and Jeschke, G. (2008) Photo-CIDNP MAS NMR beyond the T_1 limit by fast cycles of polarization extinction and polarization generation. *J. Magn. Reson. 190*, 43−51.
(32) van de Meent, E. J., Kleinherenbrink, F. A. M., and Amesz, J. (1990) Purification and properties of an antenna-reaction center complex from *Heliobacteria*. *Biochim. Biophys. Acta 1015*, 223−230.
(33) Schulten, E. A. M., Alia, Matysik, J., Kiihne, S., Raap, J., Lugtenburg, J., Gast, P., Hoff, A. J., and de Groot, H. J. M. (2002) ^{13}C MAS NMR and photo-CIDNP reveal a pronounced asymmetry in the electronic ground state of the special pair of *Rhodobacter sphaeroides* reaction centers. *Biochemistry 41*, 8708−8717.
(34) Fischer, M. R., de Groot, H. J. M., Raap, J., Winkel, C., Hoff, A. J., and Lugtenburg, J. (1992) C-13 magic-angle spinning NMR study of the light-induced and temperature-dependent changes in *Rhodobacter sphaeroides* R26 reaction centers enriched in [4′-C-13]tyrosine. *Biochemistry 31*, 11038−11049.
(35) Matysik, J., Alia, Hollander, J. G., Egorova-Zachernyuk, T., Gast, P., and de Groot, H. J. M. (2000) A set-up to study photochemically induced dynamic nuclear polarization in photosynthetic reaction centres by solid-state NMR. *Indian J. Biochem. Biophys. 37*, 418−423.
(36) Matysik, J., Schulten, E., Alia, A., Gast, P., Raap, J., Lugtenburg, J., Hoff, A. J., and de Groot, H. J. M. (2001) Photo-CIDNP C-13 magic angle spinning NMR on bacterial reaction centres: Exploring the electronic structure of the special pair and its surroundings. *Biol. Chem. 382*, 1271−1276.
(37) Bennett, A. E., Rienstra, C. M., Auger, M., Lakshmi, K. V., and Griffin, R. G. (1995) Heteronuclear decoupling in rotating solids. *J. Chem. Phys. 103*, 6951−6958.
(38) Diller, A., Roy, E., Gast, P., van Gorkom, H. J., de Groot, H. J. M., Glaubitz, C., Jeschke, G., Matysik, J., and Alia, A. (2007) N-15 photochemically induced dynamic nuclear polarization magic-angle spinning NMR analysis of the electron donor of photosystem II. *Proc. Natl. Acad. Sci. U.S.A. 104*, 12767−12771.
(39) Daviso, E., Prakash, S., Alia, A., Gast, P., Jeschke, G., and Matysik, J. (2010) Nanosecond-flash ^{15}N photo-CIDNP MAS NMR on reaction centers of *Rhodobacter sphaeroides* R26. *Appl. Magn. Reson. 37*, 49−63.
(40) Prakash, S., Tong, S. H., Alia, A., Gast, P., Jeschke, G., and Matysik, J. (2005) ^{15}N photo-CIDNP MAS NMR on reaction centers of *Rhodobacter sphaeroides*. In *Photosynthesis: Fundamental Aspect to Global Perpectives* (van der Est, A., and Bruce, A., Eds.) pp 236−237, Allen Press, Montreal.
(41) Matysik, J., Alia, A., Gast, P., van Gorkom, H. J., Hoff, A. J., and de Groot, H. J. M. (2000) Photochemically induced nuclear spin polarization in reaction centers of photosystem II observed by C-13-solid-state NMR reveals a strongly asymmetric electronic structure of the P-680$^{\bullet+}$ primary donor chlorophyll. *Proc. Natl. Acad. Sci. U.S.A. 97*, 9865−9870.
(42) Santabarbara, S., Kuprov, I., Fairclough, W. V., Purton, S., Hore, P. J., Heathcote, P., and Evans, M. C. W. (2005) Bidirectional electron transfer in photosystem I: Determination of two distances between P_{700}^+ and A_1^- in spin-correlated radical pairs. *Biochemistry 44*, 2119−2128.
(43) Poluektov, O. G., Paschenko, S. V., Utschig, L. M., Lakshmi, K. V., and Thurnauer, M. C. (2005) Bidirectional electron transfer in photosystem I: Direct evidence from high-frequency time-resolved EPR spectroscopy. *J. Am. Chem. Soc. 127*, 11910−11911.
(44) Lendzian, F., Bittl, R., Telfer, A., and Lubitz, W. (2003) Hyperfine structure of the photoexcited triplet state (3)P680 in plant PSII reaction centres as determined by pulse ENDOR spectroscopy. *Biochim. Biophys. Acta 1605*, 35−46.
(45) Kammel, M., Kern, J., Lubitz, W., and Bittl, R. (2003) Photosystem II single crystals studied by transient EPR: The light-induced triplet state. *Biochim. Biophys. Acta 1605*, 47−54.
(46) Müller, M. G., Niklas, J., Lubitz, W., and Holzwarth, A. R. (2003) Ultrafast transient absorption studies on Photosystem I reaction centers from *Chlamydomonas reinhardtii*. 1: A new interpretation of the energy trapping and early electron transfer steps in Photosystem I. *Biophys. J. 85*, 3899−3922.
(47) Holzwarth, A. R., Müller, M. G., Niklas, J., and Lubitz, W. (2006) Ultrafast transient absorption studies on Photosystem I reaction centers from *Chlamydomonas reinhardtii*. 2: Mutations near the P700 reaction center chlorophylls provide new insight into the nature of the primary electron donor. *Biophys. J. 90*, 552−565.
(48) Prokhorenko, V. I., and Holzwarth, A. R. (2000) Primary processes and structure of the photosystem II reaction center: A photon echo study. *J. Phys. Chem. B 104*, 11563−11578.

(49) Holzwarth, A. R., Müller, M. G., Reus, M., Nowaczyk, M., Sander, J., and Rögner, M. (2006) Kinetics and mechanism of electron transfer in intact photosystem II and in the isolated reaction center: Pheophytin is the primary electron acceptor. *Proc. Natl. Acad. Sci. U.S.A. 103*, 6895−6900.

(50) Alia, Roy, E., Gast, P., van Gorkom, H. J., de Groot, H. J. M., Jeschke, G., and Matysik, J. (2004) Photochemically induced dynamic nuclear polarization in photosystem I of plants observed by C-13 magic-angle spinning NMR. *J. Am. Chem. Soc. 126*, 12819−12826.

(51) van Brederode, M. E., van Mourik, F., van Stokkum, I. H. M., Jones, M. R., and van Grondelle, R. (1999) Multiple pathways for ultrafast transduction of light energy in the photosynthetic reaction center of *Rhodobacter sphaeroides*. *Proc. Natl. Acad. Sci. U.S.A. 96*, 2054−2059.